ISSN 1063-7761, Journal of Experimental and Theoretical Physics, 2020, Vol. 130, No. 5, pp. 673–680. © Pleiades Publishing, Inc., 2020.
Published in Russian in Zhurnal Eksperimental'noi i Teoreticheskoi Fiziki, 2020, Vol. 157, No. 5, pp. 805–813.

SOLIDS AND LIQUIDS

First-Principles Study on PdMnSn and PtMnSn Compounds in $C1_b$ Structure

Nihat Arıkan[a,*], Yasin Göktürk Yıldız[b,], and Gökçen Dikici Yıldız[c]**

[a] *Department of Mathematics and Science, Education Faculty, Ahi Evran University, 40100 Kırşehir, Turkey*
[b] *Department of Electronics and Automation, Kırıkkale University, 71450 Kırıkkale, Turkey*
[c] *Department of Physics, Faculty of Arts and Sciences, Kırıkkale University, 71450 Kırıkkale, Turkey*
** e-mail: narikan@ahievran.edu.tr*
*** e-mail: gokturk@kku.edu.tr*

Received June 9, 2019; revised September 8, 2019; accepted September 20, 2019

Abstract—The phase stability, the electronic, mechanic and lattice dynamical properties of $C1_b$-type PdMnSn and PtMnSn compounds were investigated using first principles density functional calculations within the generalized gradient approximation. The computed lattice constants of PdMnSn and PtMnSn compounds were in line with the experimental and theoretical data in the published literature. The elastic constants in the $C1_b$ structure for PdMnSn and PtMnSn compounds were carried out using the energy-strain method. The computed values of three independent elastic constants, both compounds are mechanically stable in the $C1$-type crystal structure and met the stability criteria. The electronic structure, total and partial density values of states, and total magnetic moment of these compounds were calculated and the evaluations were carried out by comparing with the existing results. Dynamic properties of PdMnSn and PtMnSn compounds were obtained using the density functional perturbation theory. Both of the compounds were dynamically stable due to the absence of the imaginary phonon frequencies. In addition, it was found that the compounds had a rapid rise in specific heat capacities from 0 to 300 K.

DOI: 10.1134/S1063776120050015

1. INTRODUCTION

Triple Heusler alloys have two separate families; one of which is the complete Heusler alloys that crystallize in the $L2_1$ structure and has the X_2YZ formula [1]. The second family is the half-Heusler alloys, whose general formula is XYZ and crystallizes in the form of AlLiSi ($C1_b$) [2–4]. Here, X is a typical heavy transition metal; Y is a rare earth or a transition metal, while Z is the main group element. The structural, phase transition, electronic band structure, chemical bonding, charge density, charge transfer and mechanical properties of PtMNSn were investigated in various studies, adopting various experimental and theoretical approaches [5–19]. The structural and magnetic properties of the PtMnSn compound were measured by means of X-ray, magnetic and NMR methods described by Watanabe [5]. De Groot et al. [6] measured the magnetic moment of PtMnSn and other $C1_b$ compounds. Crystal structures and magnetic properties of PtMnSn compound were investigated by means of X-ray and magnetic analyses [7]. Lindgren et al. [8] measured the hyperfine fields for PtMnSn compound with the time differential PAC technique. For PtMnSn disordered ferromagnets, X-ray powder diffraction, magnetization and Mössbauer measurements were carried out by Görlich et al. [10]. Galanakis et al. [11] method the X-ray magnetic circular dichroism and the electronic structure for PtMnSn compound by the LMTO method. The electronic structure, chemical bonding, charge density, charge transfer and magnetic properties of PtMnSn compound were investigated using the TB-LMTO-ASA method by Offernes and Kjekshus [12]. Structural stability, electronic, elastic constants, phase transition and magnetic properties of PtMnSn compound were studied using VASP code by Amudhavalli et al. [13]. In addition, the electronic band structure and elastic properties of the PtMnSn compound were obtained by VASP-GGA calculations [14, 15]. Otto et al. [3] measured the crystal structure, the microstructure and magnetic properties of PtMnSn compound. The crystallographic, Curie temperature and the magnetic properties of Mn-based PtMnSn compound were reported by van Enge et al. [16]. The Curie and Neel temperatures, magnetic moments, electrical resistivity, plasma frequency, relaxation frequency, and optical resistivity of PtMnSn compound in the $C1_b$-type crystal structure were reported by Kirillova et al. [17] The data available for the PdMnSn compound was very few. Şaşıoğlu et al. [18] studied spin projected electronic band structure of PdMnSn in the $C1_b$ phase using the augmented

spherical wave method. The phonon properties are important to understand the dynamic properties of solids. The phonon properties are necessary to understand the physical properties including phase transition, thermodynamic stability, transport and thermal properties. According to the literature research, there is no data available on the investigation of phonon properties of both compounds. In an effort to understand them in the present study, ab initio calculations were performed to examine the ground state properties of PdMnSn and PtMnSn compounds in the $C1_b$ phase including lattice constant, electronic band structure, elastic, thermodynamic, phonon properties, and ductility as well.

2. CALCULATION METHOD

Ab initio calculations were performed using the computer software Quantum-ESPRESSO [19]. In the present study the Perdew–Burke–Ernzerhof (PBE) [20] was adopted for the exchange-correlation potential. The wave functions were expanded in a plane-wave basis set with a kinetic energy cut-off of 40 Ry for $C1_b$ structure. The electronic charge density was evaluated up to the kinetic energy cut-off of 400 Ry.

Convergence threshold was taken 10^{-9} Ry with mixing beta of 0.7 so that results will appropriately precise. Energy convergence of 1 mRy per atom has been met by using $10 \times 10 \times 10$ Monkhorst–Pack [21] grid of k-points for sampling of the full Brillouin zone.

To find full phonon dispersions and the density of states, eight dynamical matrices were determined on a $4 \times 4 \times 4$ q-point mesh. Fourier deconvolution was used to assess the dynamical matrices at arbitrary wave vectors. From computed phonon frequencies and DOS, the constant-volume specific heat (C_V) versus temperature was determined with a quasi-harmonic approach (QHA) [22].

One way to obtain important information about the mechanical and dynamic properties of materials is from the elastic constants. There are three independent elastic constants for a cubic material (C_{11}, C_{12} and C_{44}). The three elastic constants were used to determine an energy difference between distorted and undistorted lattice-cell. Firstly, the elastic constants can be computed and then related crystalline properties such as bulk modulus (B), shear modulie (G), Young's modulus (E) can be acquired. Here, the bulk modulus is determined as a measure of how resistant a material is under compression under applied pressure and given as follows;

$$B = (C_{11} + 2C_{12})/3. \quad (1)$$

The shear modulus indicated by G is defined as the ratio of shear stress to shear strain:

$$G = (C_{11} - C_{12} + 3C_{44})/5. \quad (2)$$

The Young modulus (E) is calculated from the material's Bulk modulus and Shear modulus and is an indication of the hardness for the materials and given as follows;

$$E = \frac{9BG}{3B + G}. \quad (3)$$

Anisotropy factor (A) for crystals of cubic symmetry defined the degree of anisotropy compared to isotropic material, which is thought to have a significant impact on engineering science:

$$A = \frac{2C_{44}}{(C_{11} - C_{12})}. \quad (4)$$

The Poisson's ratio (σ) gives detailed information regarding the bonding nature of a material and is defined as the rate of extension of the lateral contraction:

$$\sigma = \frac{1}{2}\left(1 - \frac{E}{3B}\right). \quad (5)$$

3. RESULTS AND DISCUSSION

The studied PdMnSn and PtMnSn compounds in the half-Heusler phase were crystallized in the $C1_b$ phase corresponding to the space group $F43m$ (no. 216). The $C1_b$-type structure and orientations of Mn atomic spins along c-axis of PdMnSn and PtMnSn compounds, which includes one molecule with three atoms per unit cell, is presented in Fig. 1. Thus, the structural information of a material can be completely defined by the lattice parameter a. To determine the structural characteristics of PdMnSn and PtMnSn compounds, the calculations of the total energies were carried out as a function of lattice parameters. The calculated total energies were fitted to the Murnaghan's equation of state [23] to determine the structural properties, such as lattice constant (a), bulk modulus (B) and its pressure derivative (B'). The computed structural parameters of PdMnSn and PtMnSn compounds are summarized in Table 1 and a comparison was made, with the present data. The lattice a constant, bulk modulus and their pressure derivative are given and compared in Table 1, in addition to the published experimental and theoretical studies [5–13]. In any case, most of theoretical results, although obtained using different computational approaches, accurately predict the experimental lattice parameter, which varies over a rather broad range of 6.129 to 6.264 Å. The lattice constant calculated for PtMnSn compound was smaller than the experimental values. In case of GGA, the lattice parameter was higher than the experiment. However, for Pt-based compounds, especially when substituted such as Sn, Sb, and Te, valence electrons were slowly added to the system, thus a decrease in the lattice parameter was observed [11]. Very similar to the results discussed for TiNiSn, LDA and GGA fairly underestimate lattice parameter

whereas experimental values exhibit the opposite trend and overestimates it [25]. To investigate the total magnetic moments of PdMnSn and PtMnSn compounds, we computed the total magnetic moments of these compounds. The total magnetic moment of the Heusler alloys follows a simple rule known as the Slater-Pauling behavior (SP): Mt = Zt – 18 [24], where Zt is regarded as the total valence counts of electrons per unit cell. The total electron counts of Zt was determined by the sum of spin majority (up) and spin minority (down) electrons. So the determined Zt is as follows;

$$\begin{gathered} Zt = N\uparrow + N\downarrow \quad \text{and} \\ Mt = N\uparrow - N\downarrow \rightarrow Mt = Zt - 2N\uparrow \end{gathered} \tag{6}$$

The computed total magnetic moment values were found to be $3.61\mu_B$ and $3.591\mu_B$ for ferromagnetic PdMnSn and PtMnSn, respectively, and were in line with the SP rule. The computed total magnetic moments along *c*-axis are given in Table 1 along with the comparison of the current experimental and theoretical values [5–17].

The elastic constants are quantities characterizing mechanical properties of a material, and often present important results regarding the mechanical stability. The computed values of B, C_{11}, C_{12}, and C_{44} of PtMnSn and PdMnSn compounds are summarized in Table 2 along with data from other computations for comparison [13–15]. Based on the research on published literature, no experimental and theoretical data were found for the elastic constants of PdMnSn so the present computed results for the $C1_b$ phase can serve as an estimate for the upcoming researches. Our computed values of elastic constants of PtMnSn were found to be higher than the reported values in [14, 15], and it was found to be lower than the reported values in [13]. The mechanical stability of both compounds was analyzed and evaluated by using their elastic constants. The Born criteria [26] of mechanical stability conditions for the cubic structures is as follows:

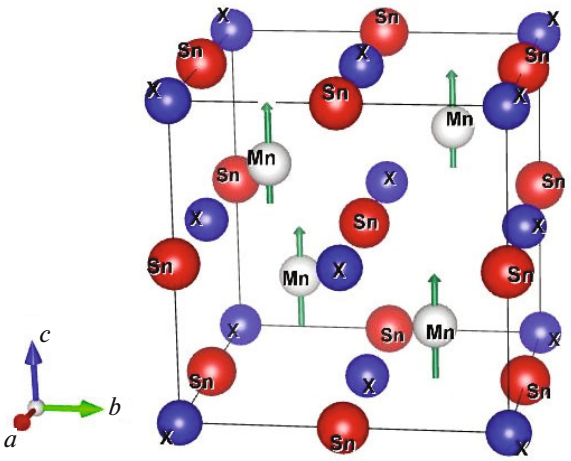

Fig. 1. (Color online) The $C1_b$-type structure of PdMnSn and PtMnSn compounds and orientations of Mn atomic spins along *c*-axis.

$$\begin{gathered} C_{44} > 0, \quad (C_{11} - C_{12})/2 > 0 \quad \text{and} \\ B = (C_{11} + 2C_{12})/3 > 0 \end{gathered} \tag{7}$$

As presented in Table 2, these criteria were confirmed, so it was concluded that both compounds were

Table 1. Calculated lattice constant a (Å), bulk modulus B (GPa) and total magnetic moment of PdMnSn and PtMnSn

Compounds	Ref.	a	B	B'	Mt(μ_B)
PdMnSn	This work	6.095	81	5.43	3.61
PtMnSn	This work	6.068	96.5	5.87	3.591
	Exp. [3]	6.261			3.50
	Exp. [5]	6.201			3.04
	Theory [6]				3.60
	Exp. [7]	6.241			3.25
	Exp. [8]				3.95
	FLAPW [9]	6.204			3.96
	Exp. [10]	6.262			3.45
	FP-LMTO [11]	6.182			3.88
	TB-LMTO-ASA [12]	6.264			3.54
	VASP [13]	6.264			3.54
	VASP [14]	6.129			3.487
	VASP [15]	6.222			3.693
	Exp. [16]	6.264			3.42
	Exp. [17]				3.57

Table 2. The calculated elastic constants (C_{ij_1}) of PdMnSn and PtMnSn

Compounds	Ref.	C_{11}	C_{12}	C_{44}	CP = ($C_{12} - C_{44}$)
PdMnSn	This work	113.339	95.630	9.290	86.340
PtMnSn	This work	139.574	110.926	12.526	98.400
	Ref. [13]	214.65	141.01	35.09	105.920
	VASP [14]	103	79	16	63
	VASP [15]	134	95	31	64

Table 3. Calculated shear modulus G (GPa), B/G, Young's modulus E (GPa), Poisson's ratio σ, anisotropy factor A for PdMnSn and PtMnSn

Compounds	Ref.	B	G	B/G	E	σ	A
PdMnSn	This work	101.533	9.113	11.141	26.547	0.45	1.05
PtMnSn	This work	120.477	13.216	9.115	38.171	0.44	0.87
	VASP [13]	129.77	35.78	3.626	98.305	0.37	0.95
	VASP [14]	87	14	6.214	39.861	0.42	0.27
	VASP [15]	108	26	3.857	72.205	0.39	1.59

mechanically stable in the $C1_b$ phase. Cauchy's pressure CP = ($C_{11} - C_{44}$) is a highly predictive character for the effective bonding of compounds. If a material shows a covalent bond character, the CP value is negative. The CP value is positive if the material has metallic bands. As seen in Table 1, the calculated CP values for both compounds were positive and had metallic band natures. According to the Pugh criterion [27], the B/G ratio is commonly used to obtain data on about the brittle or ductile of compounds. The B/G ratio for ductile materials was higher than 1.75, while for brittle materials B/G ratio was lower than 1.75 value. The bulk modulus, shear modulus, Young modulus, Poisson ratio and Anisotropy factory are given in Table 3, along with the published data for comparison [13–15]. As seen in; Table 3, according to the calculated B/G ratio, both materials had a ductile property.

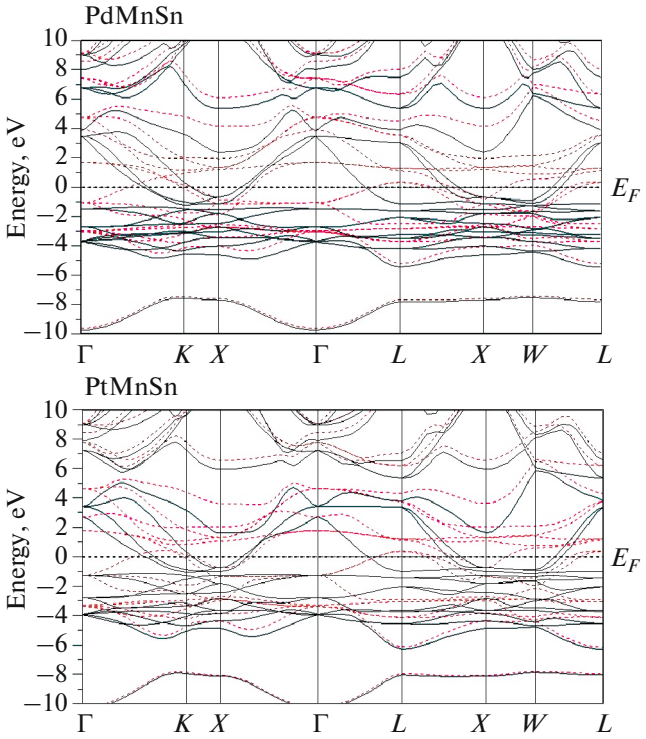

Fig. 2. (Color online) The spin polarized band profiles of PdMnSn and PtMnSn compounds.

The critical value of Poisson's ratio defines simply the crystalline bonding character in the range $0 < \sigma < 0.5$. If the Poisson ratio (σ) is smaller than $\sigma = 0.1$, the material has a covalent nature. If the Poisson ratio (σ) is 0.25, the material is in an ionic manner. According to the Poisson ratio, both compounds were found to have ionic metallic interactions. The spin dependent electronic band profiles of PdMnSn and PtMnSn compounds were employed by means of the density functional theory, within a generalized gradient approximation and displayed in Fig. 2.

As seen in Fig. 2, the Fermi levels (E_F) illustrated by a broken horizontal line of the PdMnSn and PtMnSn compounds intersected at some energy bands in the spin-up states and spin-down states. It was observed that the spin-up and spin-down electrons for both compounds had a metallic character. There were no available results published in the literature that we can compare to PdMnSn while this result was in line with the reported theoretical results for PtMnSn [11–15, 18]. As clearly seen in Fig. 2, the computed electronic band profiles of both compounds were similar to each other. To further investigate the electronic properties of these materials, the computed total den-

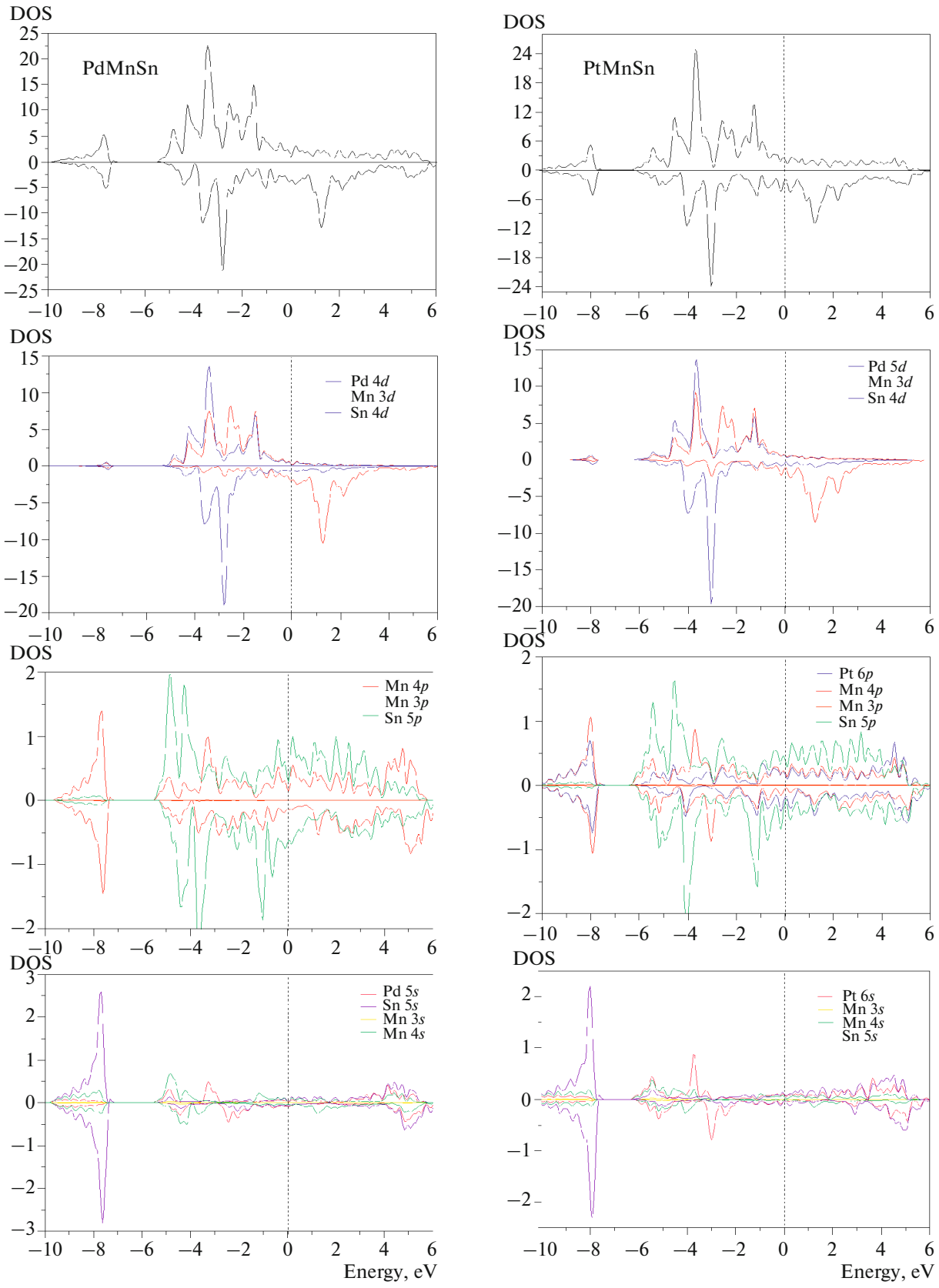

Fig. 3. (Color online) Calculated total and partial density of states for PdMnSn and PtMnSn compounds.

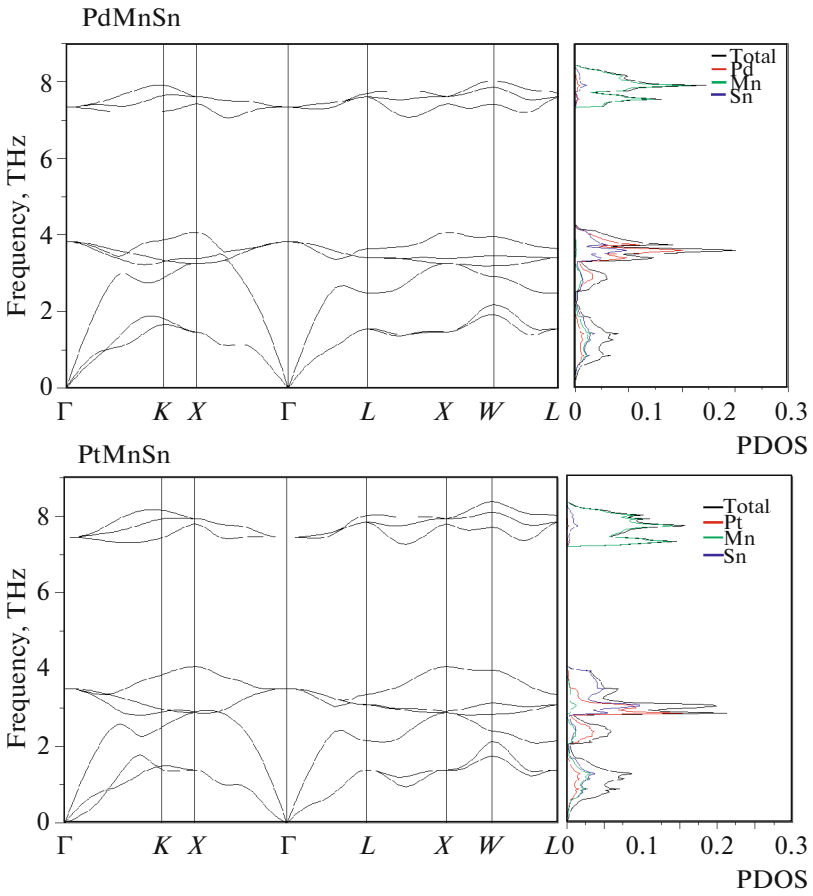

Fig. 4. (Color online) Phonon dispersion curves and phonon density of states for PdMnSn and PtMnSn compounds along several lines of high symmetry in the Brillouin zone.

sities of states and partial densities of states are shown in Fig. 3 for the present materials. The lowest bands of the energy region between −2 and −4 eV in both spin-up and spin-down states for both compounds mainly come from the *d* electrons of Pd, Pt and Mn. The lowest energy part around −8 eV for both compounds are mainly due to the *s*-states of the Sn atoms. The states lying at the Fermi level are mainly due to the Pd-4*d* (Pt-5*d*) and a small contribution from Mn-3*d* like states in PdMnSn and PtMnSn and in rest of the compounds there is also a small contribution due to Sn-*d* states. For PtMnSn these findings were in line with the reported theoretical results.

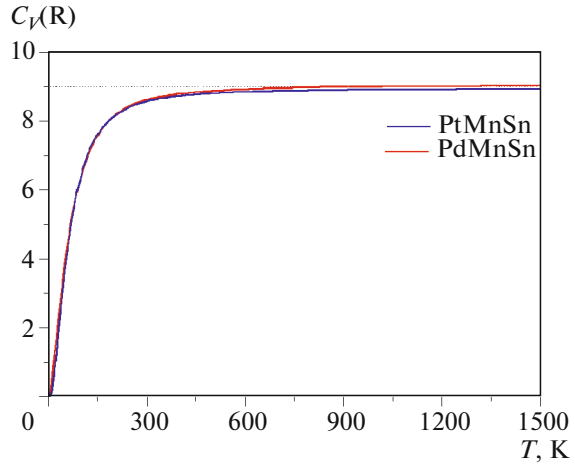

Fig. 5. (Color online) The specific heats at constant pressure versus temperature for PdMnSn and PtMnSn compounds.

The phonon spectra of the $C1_b$ phase half-Heusler PdMnSn and PtMnSn compounds along the high symmetry directions in the Brillouin zone are presented in Fig. 4. There was no imaginary phonon frequency in the Brillouin region, indicating the dynamic stability of the $C1_b$ phase of both compounds. The primitive unit cell of the half-Heusler PdMnSn and PtMnSn compounds had a total of three atoms. Thus, it consisted of a total of nine phonon branches, including three acoustic branches and six optical branches. In both of these compounds, the transverse acoustic

modes along (Γ–*X*) and (Γ–*L*) directions were twofold degenerate due to the symmetry. All phonon curves of both compounds are very similar.

The phonon spectra for both compounds can be divided into two distinct regions due to the mass difference of atoms in the primitive unit cell and have a band gap. As can be clearly seen in Fig. 4, these two regions consisted of a low frequency region between 0 and 4 THz and a high frequency region between 7 and 8 THz. For both compounds, there were nine phonon modes in the low-frequency region that extend above 4 THz. There are a total of three optic branches in the high frequency region for both compounds and these phonon branches were less dispersive than the other optical branches in the low frequency region. To better understand the nature of phonon spectra, it is necessary to look at the total phonon DOS and projected phonon DOS in Fig. 4 (right panel). The lower frequency region up to 2 THz for the two compounds was dominated by the vibrations of the three atoms due to the weak bonding forces between these atoms. For both compounds, the higher optical modes between 7 and 8 THz were dominated by the vibrations of the Mn atoms. The specific heat capacity (C_V) at the constant volume can be calculated as a function of temperature using quasi harmonic approximation (QHA). The constant volume specific heat capacity of PdMnSn and PtMnSn compounds were calculated as a function of temperature in the range 0–1500 K and presented in Fig. 5. For both compounds, a rapid increase approximately up to 300 K was observed and then it reached a level of saturation by approaching the Dulong–Petit limit [28]. Unfortunately, there were no data available in the literature for further comparison of our results.

CONCLUSIONS

The aim of this research was to determine, the structural, electronic, and vibration properties of PdMnSn and PtMnSn compounds using the density functional theory (DFT) within the generalized gradient approximation (GGA). The calculated lattice constant and bulk modulus of PdMnSn and PtMnSn compound were compared with the previous theoretical and experimental results in the published studies. The mechanical stability of both compounds were analyzed by means of elastic constants. From the analysis of the calculated elastic constants, both of the materials considered were mechanically stable. Brittleness and ductility of both compounds were studied by Pugh criteria and both compounds were found to exhibit ductile behavior. In addition, the ductility nature for the PtMnSn compound determined according to the Poisson's ratio σ were in line with the predicted results with the B/G ratio. The electronic band structures of both compounds in the $C1_b$ phase were studied and they exhibited metallic character. The calculated Cauchy's pressure CP values were positive and show the metallic band properties. The phonon spectra of the $C1_b$ phase half-Heusler PdMnSn and PtMnSn compounds along the high symmetry directions in the Brillouin zone were investigated using linear response theory. The calculated phonon spectra for both compounds confirmed dynamic stability since no images were the observed for the phonon frequency.

In addition to phonon properties, the thermodynamic properties of both compounds were investigated and analyzed. A rapid increase approximately up to 300 K was observed and then it reached a level of saturation by approaching the Dulong–Petit limit. Unfortunately, there were no data available in the literature for further comparison of our results.

REFERENCES

1. P. Villars and L. D. Calvert, *Pearson's Handbook of Crystallographic Data for Intermetallic Phases*, 2nd ed. (ASM Int., Materials Park, OH, 1991).
2. L. Offernes, P. Ravindran, C. W. Seim, and A. Kjekshus, J. Alloys Compd. **458**, 47 (2008).
3. M. J. Otto, R. A. M. van Woerden, P. J. van der Valk, et al., J. Phys.: Condens. Matter **1**, 2341 (1989).
4. M. J. Otto, H. Feil, R. A. M. van Woerden, et al., J. Magn. Magn. Mater. **70**, 33 (1987).
5. K. Watanebe, J. Phys. Soc. Jpn. **28**, 302 (1970).
6. R. A. de Groot, F. M. Mueller, P. G. van Engen, and K. H. J. Buschow, Phys. Rev. Lett. **50**, 2024 (1983).
7. M. Masumoto and K. Watanabe, Trans. Jpn. Inst. Met. **14**, 408 (1970).
8. B. Lindgren, K. Pernestal, S. Bedi, and E. Karlsson, J. Phys. F **7**, 2405 (1977).
9. S. E. Kulkova, S. V. Eremeev, T. Kakeshita, S. S. Kulkov, and G. E. Rudenski, Mater. Trans. **47**, 599 (2006).
10. E. A. Görlich, R. Kmieć, K. Łątka, et al., Phys. Status Solidi A **30**, 331 (1975).
11. I. Galanakis, S. Ostanin, M. Alouani, H. Dreyssé, and J. M. Wills, Phys. Rev. B **61**, 4093 (2000).
12. L. Offernes, P. Ravindran, and A. Kjekshus, J. Alloys Compd. **439**, 37 (2007).
13. A. Amudhavalli, R. Rajeswarapalanichamy, and K. Iyakutti, J. Alloys Compd. **708**, 1216 (2017).
14. M. De Jong, W. Chen, T. Angsten, et al., Sci. Data **2**, 150009 (2015).
15. A. Jain, S. P. Ong, G. Hautier, et al., Appl. Mater. **1**, 011002 (2013).
16. P. G. van Engen, K. H. J. Buschow, R. Jongebreur, and M. Erman, Appl. Phys. Lett. **42**, 202 (1983).
17. M. M. Kirillova, A. A. Makhnev, E. I. Shreder, V. P. Dyakina, and N. B. Gorina, Phys. Status Solidi B **187**, 231 (1995).
18. E. Şaşıoğlu, L. M. Sandratskii, and P. Bruno, Phys. Rev. B **77**, 064417 (2008).

19. S. Baroni, A. dal Corso, S. de Gironcoli, et al., QuantumESPRESSO: Open-Source Package for Research in Electronic Structure, Simulation, and Optimization. http://www.pwscf.org/. Accessed 2005.
20. J. P. Perdew, K. Burke, and M. Ernzerhof, Phys. Rev. Lett. **80**, 891 (1998).
21. H. J. Monkhorst and J. D. Pack, Phys. Rev. B **13**, 5188 (1976).
22. E. I. Isaev, QHA Project. http://qe-forge.org/qha. Accessed May 25, 2013.
23. F. D. Murnaghan, Proc. Nat. Acad. Sci. U. S. A. **30**, 244 (1944).
24. I. Galanakis, P. Mavropoulos, and P. H. Dederichs, J. Phys. D: Appl. Phys. **39**, 765 (2006).
25. M. Born and K. Huang, *Dynamical Theory of Crystal Lattices* (Oxford Univ. Press, New York, 1954).
26. S. F. Pugh, London, Edinburgh, Dublin Philos. Mag. J. Sci. **45** (367), 823 (1954).
27. A. Petit and P. Dulong, Ann. Chem. Phys. **10**, 395 (1819).
28. D. Wee, B. Kozinsky, B. Pavan, and M. Fornari, J. Electron. Mater. **41**, 977 (2012).